Characterization of Modified Polypropylene by Scanning Electron Microscopy

PETER POELT,[1] ELISABETH INGOLIC,[1] MARKUS GAHLEITNER,[2] KLAUS BERNREITNER,[2] WOLFGANG GEYMAYER[1]

[1] Research Institute for Electron Microscopy, Graz University of Technology, Steyrergasse 17, A-8010 Graz, Austria

[2] Borealis AG, St. Peterstr. 25, A-4021 Linz, Austria

Received 19 July 1999; accepted 8 February 2000

ABSTRACT: Characterizing the morphology of modified multiphasic polymer systems, as are often applied for improving the impact strength, is normally a complicated and tedious task. Nevertheless, knowledge about the volume fraction and particle-size distribution of the elastomer phase is important for the specific development of high-impact systems. Direct production in the reactor enables only indirect control of these two quantities. Computer-controlled scanning electron microscopy in combination with image processing allows an automated measurement of both all the necessary particle parameters (size distribution, shape, orientation, etc.) and the elastomer content of the material. Since bulk materials are used for the investigation, additionally, three-dimensional information about the structure of the material can be gained by simply varying the electron energy, without the necessity to resort to multiple slices. This information is especially important in the case of particles with extremely irregular shapes, as obtained, for example, by strong agglomeration of the modifier particles. The mathematical routines used for calculation of the particle-size distributions from the measured profile-size distributions cannot be applied in such cases. The method was tested for several materials with significantly different compositions, both immediately after molding and also after a subsequent thermal relaxation. © 2000 John Wiley & Sons, Inc. J Appl Polym Sci 78: 1152–1161, 2000

Key words: polypropylene; EP copolymer; image processing; particle-size distribution; scanning electron microscopy

INTRODUCTION

To improve the properties of polymeric materials, for example, their toughness and stiffness, various modifiers can be added to the polymer matrix. For the modification of polypropylene (PP), often ethylene–propylene copolymer rubber (EPR) is used. But both other olefin-based elastomers and a wide variety of mineral fillers or fibers are also suitable. The actual material properties will depend on the loading, properties, shape, size, and distribution of the modifier particles and on their bonding to the matrix.[1]

One technical advantage of the system PP/EPR is the possibility to directly produce these materials in a reactor cascade (reactor blends). Normally, the such-produced systems will consist of three phases[2]:

A—A crystalline PP matrix, which can also be a random copolymer with low content of ethylene[3];

B—A predominantly amorphous ethylene–propylene (EP) copolymer forming the shell of the dispersed elastomer particles;

C—A crystalline polyethylene (PE) phase with

Correspondence to: P. Poelt.

Journal of Applied Polymer Science, Vol. 78, 1152–1161 (2000)

incorporation of a low propylene amount forming the core of the elastomer particles.

In industrial polymerization processes, phase A will be produced in the first reactor and phases B and C simultaneously in a second reactor. More complex processes are, however, possible and allow an even wider variation of the material properties.[4]

In the literature, several studies about the impact of copolymer composition and structure on the morphology and final mechanical properties of such systems can be found.[5–9] In most cases, however, the authors used extruder blends of PP and externally synthesized EPR (as well as possibly PE) for the studies to avoid the problem of composition variation in the reactor. The comparability of these systems to reactor blends is, however, limited because of the lower compatibility and interaction between the phases.[10]

The most often used method to obtain morphological information about such systems is transmission electron microscopy (TEM).[1,10] But images taken from the ultrathin sections of the bulk material yield only profile-size distributions. Except for special cases, it is impossible to reconstruct the actual particle-size distributions from these profile-size distributions by means of stereology.[11–13] The method is limited to specimens where all particles have the same shape, irrespective of their size.[14] Additionally, a preferential orientation of nonspherical particles is not allowed. All these assumptions will be fulfilled only in rather rare cases and especially not in cases where deformation or agglomeration of particles occurred.

A possible way of overcoming these problems partially is a two-dimensional TEM analysis based on cuts in two directions (e.g., parallel and normal to the flow direction in an injection-molded sample). This technique allows one to reconstruct the shape and orientation of the dispersed particles at least qualitatively.[15]

An additional assumption in using stereological principles is that the sections of the specimens represent true planes, that is, that the thickness of the TEM specimens is approximately zero. Whenever the particle diameters, or at least a part of them, are of a size comparable to the thickness of the sections, a correction factor for the section thickness has to be applied.[16] But these correction factors are themselves dependent on the particle shapes and their profile diameters. Thus, they would have to be determined separately for each new system.

To get a direct projection image of the particles, the technique of high-voltage TEM (HVEM) also can be used. Here, an investigation of thicker samples (cuts up to a thickness of a few micrometers) is possible due to the high acceleration voltage (max. 1000 keV).[17] This allows one to see at least the outline of complete particles up to a certain size. Inherent to the technique is, however, the danger of specimen damage because of the high-energy input.

Gleinser et al. showed for spherical particles that, with an increasing ratio of slice thickness to particle diameter, the profile-size distribution approaches more and more the actual particle-size distribution.[11] Especially, the calculated mean particle diameters are nearly equal already at moderate ratios. Scanning electron microscopy (SEM), which is generally performed on bulk specimens, offers the possibility to vary the penetration depth of the electrons and with it the information depth, in a broad range. Thus, in the case of small particles, the "specimen thickness"-to-particle diameter ratio can be varied correspondingly. Additionally, in the case of very irregularly shaped particles, it is often possible to elucidate the particle shape without the necessity to resort to serial section methods. Although confocal scanning laser microscopy is used more and more to study the morphology of polymer blends, its resolution is by far inferior to that of field-emission SEM.[18] This method is furthermore limited to materials which are transparent for the respective laser wavelength. In the following sections, the possibility to use SEM and subsequent image processing for both particle characterization and the determination of the particle-size distribution of two-phase polymer systems is demonstrated.

EXPERIMENTAL

Materials

Four different grades of heterophasic EP copolymers (see Table I) with different amounts and compositions of the EPR modifier were chosen for the investigation, which was conducted both on freshly molded and thermally relaxed specimens. All materials were produced in pilot-scale or commercial-scale reactors at Borealis AG (Schwechat, Austria). While the materials CSC and DSC are

Table I Basic Characteristics of the Investigated Materials

Material	07	09	CSC	DSC
MFR (g/10 min)	8	8	2	4
C2 total (mol %)	30	17	12	16
XS (wt %)	36	17	14	25
Flexural modulus (MPa)	480	850	1100	880
Charpy + 23°C/kJ/m^2	65	16	19	28
Charpy − 20°C/kJ/m^2	8.5	2.8	5.5	6.3

MFR according to ISO 1169 Standard—230°C/2, 16 kg, C2 from infrared spectroscopy, and XS according to internal method. Flexural modulus according to ISO 178 standard and Charpy notched impact strength according to ISO 179 1eA standard.

standard high-impact copolymers, the experimental grades 07 and 09 were produced with the target of a finer elastomer particle structure by adapting both the phase composition (propylene-rich EPR and random copolymer matrix) and the phase viscosities to each other. This way, products with an improved balance between transparency and impact strength can be achieved.[3,19] The total ethylene (C2) content, melt flow rate (MFR), and other basic data for the grades are given in Table I.

For the study, standard mechanical testing specimens (80 × 10 × 4 mm) were injection-molded. These were the basis for the "molded" investigations. The thermal treatment for a relaxation of the particle shape, which may be strongly oriented and deformed in the molding step, was carried out in accordance with the work of Mirabella.[20] The specimens were heated in a vacuum to roughly 2°C above the melting point of the matrix and left at this temperature for 20 min, followed by a slow cooling to room temperature. In most cases, this led to a distortion of the external specimen shape, pointing to internal stresses created in the molding step.

Preparation

RuO_4 Staining for TEM and SEM

As polymer matrix and modifier particles have approximately the same chemical composition and density, the particles are not visible in electron microscopy without a preceding preparation. Square-shaped specimens were trimmed into a pyramid shape and then at the tip a flat surface was produced with a glass knife. Subsequently, the specimens were stained by gaseous RuO_4.[21] The continuous Ru layer formed at the surface was removed by ultramicrotomy. Staining made the material brittle, thus preventing the danger of smearing or particle deformation in the cutting process.

Chemical Etching for SEM

The specimens were—like those for staining—trimmed; then a flat surface was produced by cryomicrotomy at the tip. Etching was performed in *n*-hexane at 60°C for 20 min.[20] The EPR phase is etched much stronger than is the PP matrix and, thus, removed, but only in those cases where the particles have direct contact with the surface.

Instrumentation

The SEM pictures were recorded and processed by a Noran Voyager image-processing system attached to a Zeiss DSM 982 Gemini field-emission SEM with either a resolution of 1024 × 1024 or 1280 × 1024 pixels. The electron energy at the SEM is variable between 0.2 and 30 keV. As the Noran Voyager also controls the motorized specimen stage, a fully automated recording and processing of as many images as necessary is possible. TEM pictures were recorded by a Philips 300, subsequently digitized and also processed by the Noran Voyager.

To eliminate the influence of noise, only structures with an area of at least 30 pixels were evaluated. Additionally, it is impossible to get reliable profile shape data from profiles with an area of a few pixels only. Comparisons of profile distributions have—if not stated otherwise—always been scaled to the same area, even if the actually evaluated areas had been different in size (e.g., because of different magnifications). Statistical errors will in these cases also be different.

The average diameter is defined as the average of all triangle altitudes drawn between pixels on the convex perimeter. Triangle bases are defined by adjacent pixels, and peaks, by pixels on the opposite side. The resolution in the average diameter in the digitized size distributions is always 0.1 μm.

RESULTS

SEM Parameters and Particle Imaging

Contrary to TEM, where slices with a thickness of around 50–100 nm are usually investigated, in

Table II Dependence of the Penetration Depth of the Electrons on the Electron Energy (ρ = 1 g/cm^3)

E_0 (keV)	D_P (μm)
1	0.1
2	0.3
5	1.0
10	2.6
15	6.2
20	10.0
25	14.5

The maximum information depth in case of backscatter electrons is around half the penetration depth.

SEM, normally bulk specimens are analyzed. The penetration depth D_p of electrons is

$$D_p \approx E_0^n/\rho$$

with E_0 being the primary electron energy, ρ being the density of the material, and the exponent $n \approx 1.4$ for low and $n \approx 1.7$ for high energies.[22,23] Rough estimates for the penetration depth as a function of the energy are given in Table II. The actual information depth is around half of it, because the electrons have to leave the specimen again to be collected by the detector.

Table II shows that at an energy of 1 keV the information depth is comparable to the thickness of the TEM slices and that the information depth can be varied by a factor of 100. Brown and Butler proved that even at energies as low as 1 keV images of RuO_4-stained PE blends can be recorded with excellent contrast.[24] In Figure 1, the change of the particle size, shape, and number in dependence on the primary electron energy is demonstrated for the specimen with the most irregular particle shapes. One perceives immediately the existence of an inverse relationship between particle density and the maximum applicable information depth—the greater is the former, the smaller is the latter. Otherwise, the images of particles of different depths begin to overlap and the individual particles cannot be discriminated clearly any longer. RuO_4 staining occurred to a sufficient depth and did not limit the depth variation.

At the regions marked A and B in Figure 1, one can easily follow the change in particle shapes with increasing electron energy. What seem to be individual particles at 5 keV turn out to be parts of greater agglomerates at higher energies. Of course, the narrow bridges between the bigger

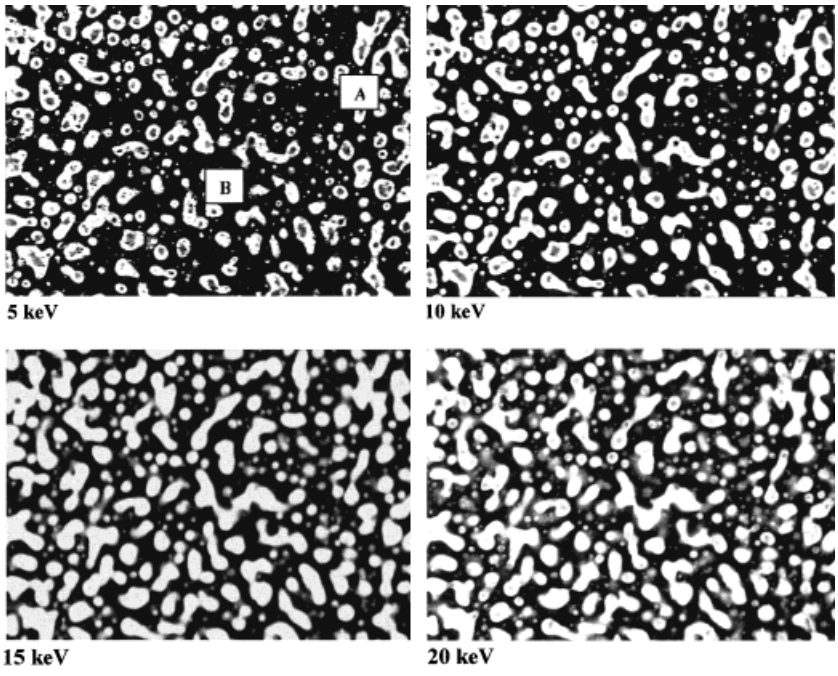

Figure 1 Dependence of particle shapes and sizes for material 07 on the electron energy used in SEM (BSE detector, picture width: 39 μm).

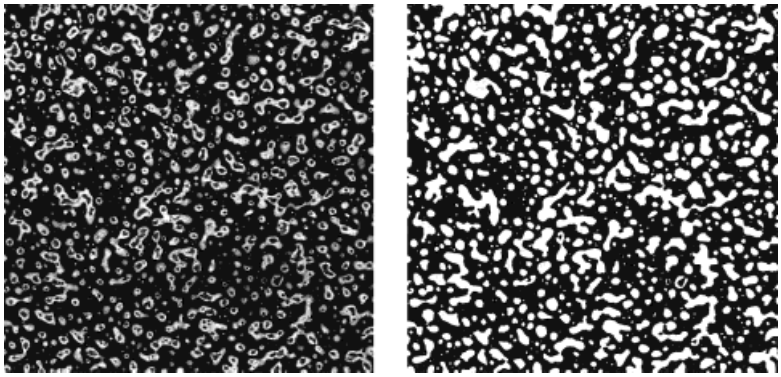

Figure 2 Structure of material 07 after thermal relaxation (picture width: 57 μm); (left) original SEM image (5 keV, BSE detector); (right) after binarization and holefill procedure.

parts of the dumbbell-like agglomerates have a much lower probability to be cut and to be directly visible at the surface than that of the great spherical parts of the same agglomerate. Thus, in ultrathin sections for TEM, agglomeration could be strongly underestimated and the number of small particles counted too high. Also, the aforementioned algorithms for reconstructing the particle-size distribution from the profile-size distribution are not applicable in this case.

What appears to be agglomerates could also, at least in some cases, be the overlap of particle images from particles at different depths. For individual particles, this could be checked by tilting the specimen to a high angle. Selective etching of the specimen, where the EPR phase was removed, proved, however, also the existence of these highly irregular agglomerates. But because the contrast at the boundaries of the etched holes is not sufficiently different from that of the matrix, the etched specimens are not suited for an automated profile-size distribution measurement.

Connected with the finite section thickness is always—both in SEM and TEM—the loss of cap sections.[16] For particles, which are contained in a slice with a shallow cap section, the contrast between this cap and the matrix may be too weak to make it visible in the recorded image. The size of these invisible caps is dependent on the ratio of electron penetration depth to cap depth and will, therefore, increase with increasing electron energy in the SEM. Additionally, as demonstrated in Figure 1, particles from greater depths are recorded with a fainter contrast. This is a consequence of a scattering of the electrons on their way back to the surface. It provides a rough depth discrimination without switching to lower energies. But, as a consequence, also the minimum particle and cap sizes detectable increase. Thus, there is a correlation between the electron energy and the minimum detectable profile size. But, in effect, this causes a shift of the profile-size distribution in direction of the actual particle-size distribution.

A problem omnipresent in connection with polymers and SEM is the danger of specimen damage caused by the electron beam. Because of the low heat conductivity of polymers, substantial heating can occur and, as a consequence, chemical degradation and a change of the surface structure. The greater the electron energy and the magnification, the higher is the danger of damage. It did not pose a problem in the present investigation, although surface roughening was observed after longer irradiation of the same area.

Profile-size Distribution Measurements

Automated discrimination of the particle profiles and measurement of their geometrical parameters (area, average diameter, circularity, orientation, etc.) uses the different gray levels of the RuO_4-stained EPR phase and the PP matrix in the SEM image. The gray-level image is converted to a binary image and subsequently processed to enhance the features. In Figure 2, a comparison of an original image with its processed counterpart is presented. Of course, the gray value chosen for image segmentation and also the subsequent processing will influence the recorded size and shape of the particles and, in the end, their size distribution. Figure 3, however, proves that the dependence of the results on

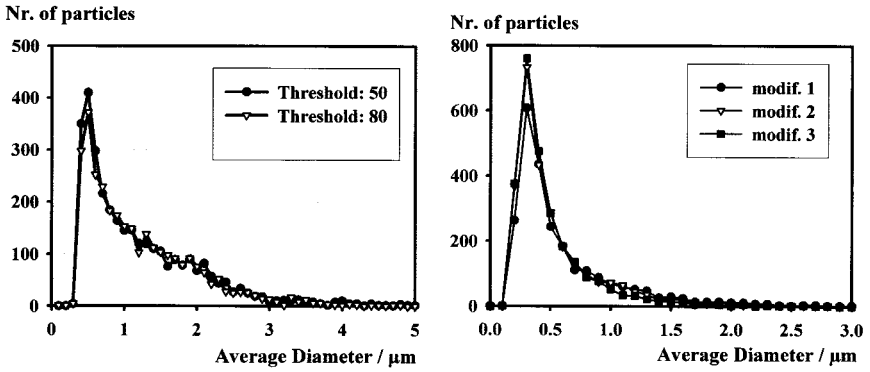

Figure 3 Dependence of the profile-size distribution on image processing and magnification; (left) material CSC, variation of the threshold value for binarization; (right) material 07, modification 1: magnification 10,000×, holefill; modification 2: magnification 10,000×, holefill, erode (twice), template separate (twice); modification 3: magnification 3.000×, holefill.

the image-processing procedure and also the magnification of the recorded images is rather small. The higher the contrast in the original image, the less image processing is necessary, reducing even more its influence.

Although at 5 keV the information depth in SEM is rather moderate (see Table II), it is, nevertheless, a multiple of the thickness of a TEM slice. Thus, a change in the profile-size distribution should already be observable. This is confirmed by Figure 4; there is no measurable shift in the peak position of the distribution and the overall shape does not change substantially, but one can notice a definite reduction in the number of small particles. The main reason may be the better perception of agglomeration by SEM, although it is still underrated even at an electron energy of 5 keV, as is proven by Figure 1. Since the smallest areas measured comprise at least 30 pixels, differences in noise or sensitivity between the two devices should not play a decisive role.

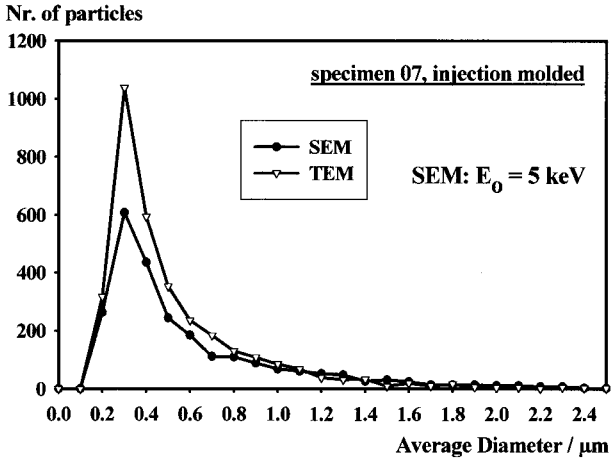

Figure 4 Comparison of the profile-size distribution for material 07 measured by SEM (5 keV) and TEM.

Shape and Orientation Parameters

In addition to the size distribution, particle-shape parameters and particle orientation can also be measured, provided that all images evaluated for a single specimen are recorded from a connected surface. Images of different slices, which are rotated or tilted against each other, are, of course, not suited. In Figure 5, an example is given for one of the specimens (material 09; both molded and thermally relaxed). Whereas the circularity of the particles does not differ decisively before and after thermal relaxation, the relaxation process erased the pronounced orientation of the EPR phase induced by the injection-molding step. The most probable reason for this is a particle-agglomeration process, not only a random rotation of the individual particles. This is supported by the strong reduction in particle number after the relaxation, as can be seen in Figure 5(a). But the circularity distribution definitely proves the particles not be spherical, so that a reconstruction of the particle-size distribution from the profile-size distribution is not possible.

DISCUSSION

While in extruder blends the relative amount of the elastomer phase can be controlled directly

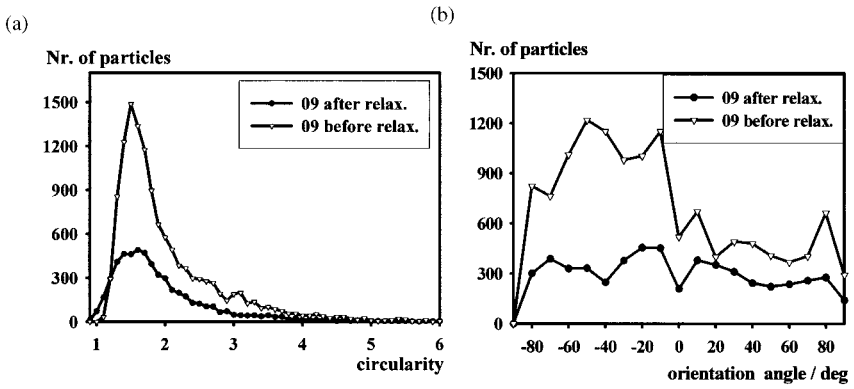

Figure 5 Comparison of (a) circularity [C = perimeter^2/(4 π area)] and (b) orientation (angle between positive X-axis and maximum particle projection) for material 09 before and after thermal relaxation.

and the particle size at least indirectly by appropriate selection of the phase viscosities,[19,25,26] both will be a complex function of the parameters of the polymerization process for reactor blends. Two generally accepted measures for the elastomer phase amount are the relative amount of polymer produced in the second reactor (W_2) and the amount of solubles in cold xylene (XS) determined by dissolving the sample completely in boiling xylene and precipitating the insoluble part by cooling slowly to room temperature again.[4] The latter quantity is given in Table I for the investigated systems. Despite its popularity in industrial practice, it has several systematic drawbacks: While it will also include matrix material of low isotacticity (through which also the XS value of homopolymers is not zero), it will not register crystalline PE fractions present in the core of the elastomer particles and contributing to the toughening process.[9] Therefore, an independent determination of the elastomer phase content through SEM will be interesting.

This is even more true for the particle-size distribution, which is not accessible otherwise. As several authors have stated a strong connection between particle size and the toughening effect,[1,10,27] detailed information about the consequence of the alteration of polymerization parameters on the morphology are of greatest interest in the systematic development of high-impact PP grades.

In Figure 6, the results of the size-distribution measurement for all four materials, both before and after thermal relaxation, scaled to the same area, are presented. Because of the different amount of EPR in the individual grades, a scaling

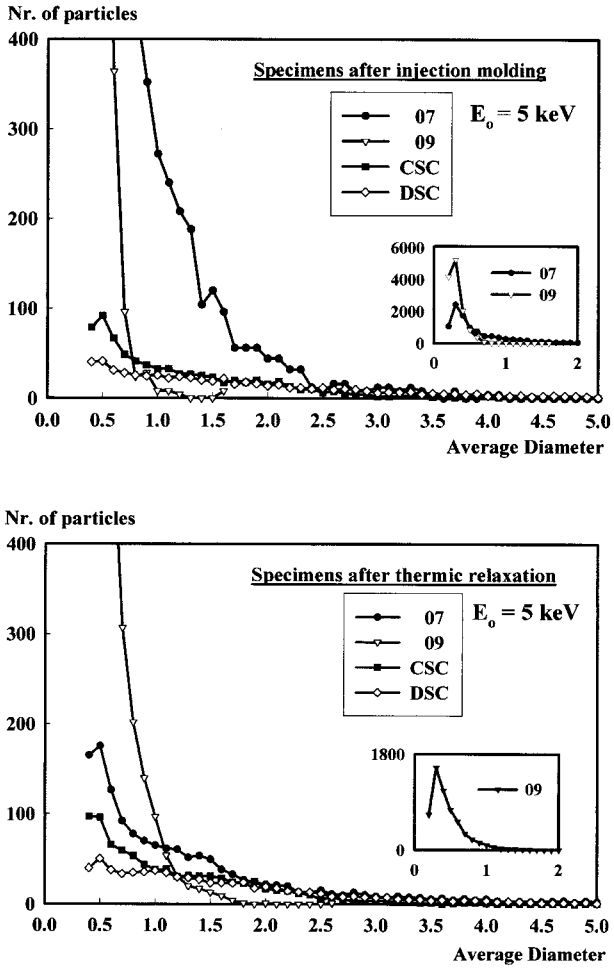

Figure 6 Particle-size distributions for all four materials before and after thermal relaxation, scaled to the same surface area.

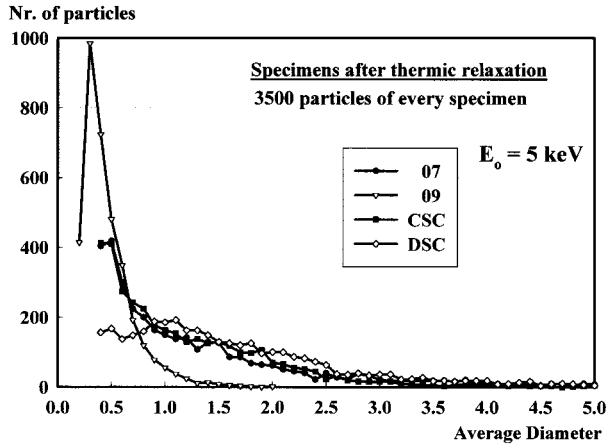

Figure 7 Profile-size distribution of the materials after thermal relaxation, scaled to the same particle number.

Table III Elastomer Content as Determined by Different Methods (No Thickness Correction for the SEM and TEM Values Applied)

Material	XS (wt %)	SEM (vol %)	TEM (vol %)
07, molded	36	34	31
07, relaxed	36	33	—
09, molded	17	11	—
09, relaxed	17	12	—
CSC, molded	14	14	—
CSC, relaxed	14	15	—
DSC, molded	25	28	—
DSC, relaxed	25	25	—

to the same particle number as presented in Figure 7 might be more favorable. This will depend on whether only the individual particle parameters are of interest or the particle density also. Figure 7 shows a great similarity in the elastomer particle-size distribution between materials CSC and 07 after thermic relaxation, which is not as clearly visible in Figure 6. Thus, for the material 07, the initially finer particle structure compared

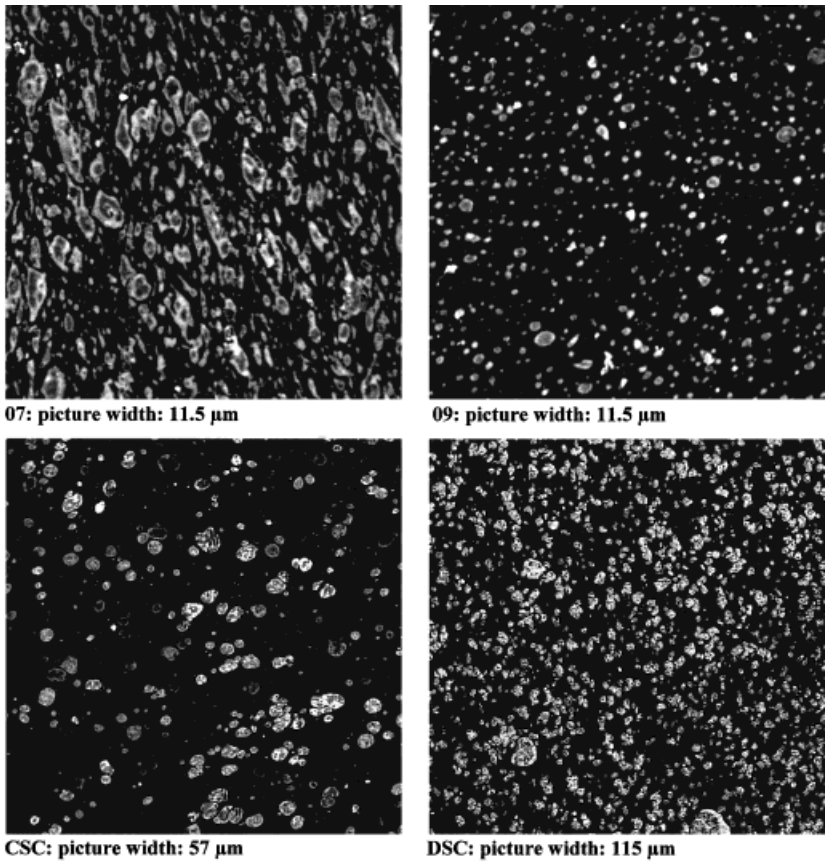

Figure 8 Elastomer-phase distribution of all four materials after injection molding for visual comparison (5 keV, BSE detector).

to the materials CSC and DSC has disappeared after the thermic relaxation. Only the material 09 preserved a substantial amount of the fine modifier particles. Comparison of the size distributions in Figure 6 demonstrates a drastic reduction in particle number per unit volume for the materials 07 and 09 after thermic relaxation. Thus, extremely strong agglomeration occurred (see also Fig. 5). Because a particle with a diameter of 5 μm has the volume of 1000 particles with a diameter of 0.5 μm, this agglomeration causes no visible change of the size distribution of the great particles. Thermic relaxation did not change the size distribution for the materials CSC and DSC substantially.

Additionally, in Table III, the elastomer-phase content as determined via XS and measured by electron microscopy are compared. In case of material 07 (molded), the content was calculated from TEM as well. As a consequence of the greater specimen thickness ($\approx$1 μm; see Table II), the value measured by SEM is higher than is the corresponding one by TEM (see also Fig. 4). Applying the thickness correction factor as proposed by Weibel[16] would give an elastomer fraction of only 21%. Since the elastomer content is, of course, the same before and after thermic relaxation, the deviation of the corresponding measurements by SEM will act as an indicator for the measurement error.

Based on the assumption that the density of the elastomer phase is about 0.85 g/cm^3, the elastomer content measured by SEM is generally smaller than that determined by XS. An especially strong difference was observed for the material 09. Aside from errors in the XS values, one explanation might be that the scanned surface area was too small. If only very few great particles are present in the matrix, then their contribution to the elastomer content could be strongly underrated. The scanned surface area has to be great enough to give a sound size distribution up to the greatest particles, even if their influence on the modification of the properties of the polymeric material would be negligible.

Figure 8 finally gives an optical survey of the elastomer-phase distribution of the four samples after injection molding. A quick glance at the structures in comparison to the quantification in Figures 6 and 7 as well as Table III makes the problem of "visual" judgment of a heterophasic system fully clear. Especially in case of high EPR content, the image can be very deceiving.

As the samples selected for this investigation do not—unlike the work by Starke et al.[10]—represent a systematic series with the variation of only one parameter, a direct correlation between the morphological information and the mechanical characteristics given in Table I could not be expected. A comparison shows, however, that the elastomer-phase content correlates much better with the impact strength than does the total C2 content, which is still frequently used for characterization of high-impact copolymers. Molar mass effects, however, disturb this simple correlation. For detecting the influence of the particle-size distribution, at least two samples with identical total elastomer content would be required.

Nevertheless, the results prove that a combination of SEM and image processing is a powerful tool for the characterization of modified polymers. The possibility of complete automation can save a lot of time, and by variation of the electron energy also to a certain amount, three-dimensional information can be gained without the necessity of using multiple slices.

The authors thank Dr. D. Leistner of Borealis AG for preparing the experimental-grade samples as well as Dr. W. Neißl of Borealis AG and Dr. C. Paulik of Borealis SA, Norway, for helpful discussions.

REFERENCES

1. Kim, G. M.; Michler, G. H.; Gahleitner, M.; Fiebig, J. J Appl Polym Sci 1996, 60, 1391–1403.
2. Schwager, H. In Proceedings of the Polypropylene World Congress 1992; Maack Business Services: Zürich, 1992; pp II-4.1–II-4.18.
3. Paulik, C.; Gahleitner, M.; Neißl, W. Plast Eur 1996, 86, 16–17.
4. Polypropylene Handbook; Moore, E. P., Ed.; Hanser: Munich, 1996; 89–98.
5. Karger-Kocsis, J.; Kallo, A.; Szafner, A.; Bodor, G. Polymer 1979, 20, 37–43.
6. Hodgkinson, J. M.; Savadori, A.; Williams, J. G. J Mater Sci 1983, 18, 2319–2336.
7. Coppola, F.; Greco, R.; Martuscelli, E.; Kammer, H. W. Polymer 1987, 28, 47–56.
8. D'Orazio, L.; Mancarella, C.; Martuscelli, E.; Sticotti, G. Polymer 1993, 34, 3671–3681.
9. Petrovic, Z. S.; Budinski-Simendic, J.; Divjakovic, V. J Appl Polym Sci 1996, 59, 301–310.
10. Starke, J. U.; Michler, G. H.; Grellmann, W.; Seidler, S.; Gahleitner, M.; Fiebig, J.; Nezbedova, E. Polymer 1998, 39, 75–82.
11. Gleinser, W.; Maier, D.; Schneider, M.; Weese, J.; Friedrich, Chr.; Honerkamp, J. J Appl Polym Sci 1994, 53, 39–46.

12. Ohser, J.; Nippe, M. J Microsc 1997, 187, 22–30.
13. Karlsson, L. M.; Cruz-Orive, L. M. J Microsc 1997, 186, 121–132.
14. Russ, J. C. The Image Processing Handbook, 2nd ed.; CRC: Boca Raton, FL, 1994; p 505.
15. Michler, G. H. Kunststoff-Mikromechanik; Hanser: Munich, 1992; pp 19–56.
16. Weibel, E. R. Stereological Methods; Academic: London, New York, 1980; Vol. 2, p 105.
17. Kim, G. M.; Michler, G. H. Polymer 1998, 39, 5689–5697.
18. Li, L.; Chen, L.; Bruin, P.; Winnik, M. A. J Polym Sci B Polym Phys 1997, 35, 979–991.
19. Paulik, C.; Neiβl, W. In ANTEC 98; Society of Plastics Engineers: Atlanta, GA, 1998; 2565–2569.
20. Mirabella, F. M. J Polym Sci B Polym Phys 1994, 32, 1205–1215.
21. Montezinos, D.; Wells, B.G.; Burns, J. L. Polym Sci Polym Lett Ed 1985, 23, 421–425.
22. Reimer, L. Scanning Electron Microscopy; Springer: New York, 1985; p 100.
23. Reimer, L. Image Formation in Low-Voltage Scanning Electron Microscopy; SPI Optical Engineering: Bellingham, WA, 1993; p 51.
24. Brown, G. M.; Butler, J. H. Polymer 1997, 38, 3937–3945.
25. Utracki, L. A.; Kamal, M. R. Polym Eng Sci 1982, 22, 96–114.
26. Vinckier, I.; Moldenaers, P.; Mewis, J. J Rheol 1997, 41, 705–718.
27. Wu, S., Polymer 1985, 26, 1855–1863.